Design, Syntheses, and Studies of Supramolecular Porphyrin−Fullerene Conjugates, Using Bis-18-crown-6 Appended Porphyrins and Pyridine or Alkyl Ammonium Functionalized Fullerenes

Francis D'Souza,*,† Raghu Chitta,† Suresh Gadde,† Amy L. McCarty,† Paul A. Karr,† Melvin E. Zandler,† Atula S. D. Sandanayaka,‡ Yasuyaki Araki,‡ and Osamu Ito*,‡

Department of Chemistry, Wichita State University, 1845 Fairmount, Wichita, Kansas 67260-0051, and Institute of Multidisciplinary Research for Advanced Materials, Tohoku University, Katahira, Sendai 980-8577, Japan

Received: December 28, 2005; In Final Form: February 7, 2006

Photoinduced electron-transfer processes in cis and trans functionalized bis-18-crown-6 porphyrin self-assembled with fullerene functionalized with pyridine or alkylammonium cation entities are reported. The structural integrity of the newly formed supramolecular conjugates was accomplished by optical absorption and emission, electron spray ionization mass, electrochemistry, and semiempirical PM3 calculations. A 1:2 stoichiometry of the supramolecular porphyrin:fullerene conjugates was deduced from these studies. The conjugates revealed stable "two-point"' binding involving metal−ligand coordination and alkylammonium cation−crown ether binding or only the latter type of binding depending upon the functionality of the fullerene and metal ion in the porphyrin cavity. The effect of the variation on free energy changes of charge separation and the charge recombination was achieved by varying the metal ion in the porphyrin cavity. The charge-separation rates (k_{CS}) determined from the picosecond time-resolved emission studies were generally higher for the cis bis-crown functionalized porphyrins than those of the corresponding trans ones. A comparison of the k_{CS} values reported earlier for 1:1 porphyrin−fullerene conjugates with a similar self-assembly mechanism suggested that employing a higher number of acceptor entities improves the electron-transfer rates. The calculated charge-recombination rates (k_{CR}) were 2−3 orders of magnitude smaller than the k_{CS} values, suggesting the occurrence of the charge recombination process in the Marcus inverted region. The lifetimes of the radical ion pair (τ_{RIP}) ranged between 46 and 233 ns indicating charge stabilization in the studied conjugates.

Introduction

Development of self-assembled supramolecular architectures hosting donor and acceptor entities capable of undergoing light-induced electron/energy transfer is a topic of current interest owing to their applications to light energy harvesting and electronic devices.[1−7] Although a significant amount of progress has been made in this area of research, challenges still exist in building supramolecules with defined geometry and orientation, and possessing more than one donor or acceptor entity, viz., forming triads, tetrads, etc. Building complicated supramolecular architectures with less effort, including structures that otherwise cannot be built by covalent chemistry, is another aspect of supramolecular chemistry. Noncovalent interactions comprised of ion−ion, ion−dipole, hydrogen-bond, dipole−dipole, and $\pi-\pi$ stacking interactions with energies ranging from a few to several hundred kilojoules per mole are available for building such supramolecules.[8] The occurrence of photoinduced electron transfer in these model donor−acceptor systems held by noncovalent interactions has been demonstrated in several instances.

Fullerenes, C_{60} and C_{70},[9] due to their inherent properties such as reversible, stepwise addition of up to six electrons[10] and low reorganization energy accompanying electron transfer,[11] have emerged as exceptional three-dimensional electron acceptors.[1] Macrocycles such as porphyrins, phthalocyanines, and metal polypyridyl have been successfully used as electron donors.[1] The advantage of these donors lies in the minimal structural changes when electrons are released from them. Studies performed have shown that the nature of the linker between the donor and acceptor entities controls the electronic coupling and thus small structural variations affect the overall photodynamics of charge separation.[1] However, it is often difficult to control the distance and orientation in noncovalently bound donor−acceptor systems primarily due to weak interactions and the associated equilibrium processes. We have addressed this issue by employing the "two-point" binding approach in porphyrin−fullerene dyads which resulted in dyads with defined distance and orientation.[12] Our methodology involved covalent-coordination,[12a] coordination-coordination,[12b] coordination-hydrogen bonding,[12c] and coordination-alkylammonium cation crown ether complexation[12d] approaches. In the coordination-alkylammonium cation crown ether complexation approach, zinc porphyrins were functionalized with one or four 18-crown-6 entities at different positions of the porphyrin ring. The acceptor, fullerene, was functionalized to possess pyridine and/or an alkylammonium cation entity. Two-point binding involving coordination of pyridine to zinc, and crown ether−alkyl cation complexation resulted in stable donor−acceptor dyads where the photoinduced electron-transfer processes were possible to monitor in a polar solvent, benzonitrile.[12d,13]

* Address correspondence to these author. F.D.: e-mail francis.dsouza@wichita.edu. O.T.: e-mail ito@tagen.tohoku.ac.jp.
† Wichita State University.
‡ Tohoku University.

10.1021/jp057547q CCC: $33.50
Published on Web 03/08/2006

SCHEME 1: Structures of the Bis-benzo-18-crown-6 Appended Porphyrins, 1−6, and the Fullerene Derivatives, 7 ($PyC_{60}NH_3^+$)−8 ($PhC_{60}NH_3^+$)

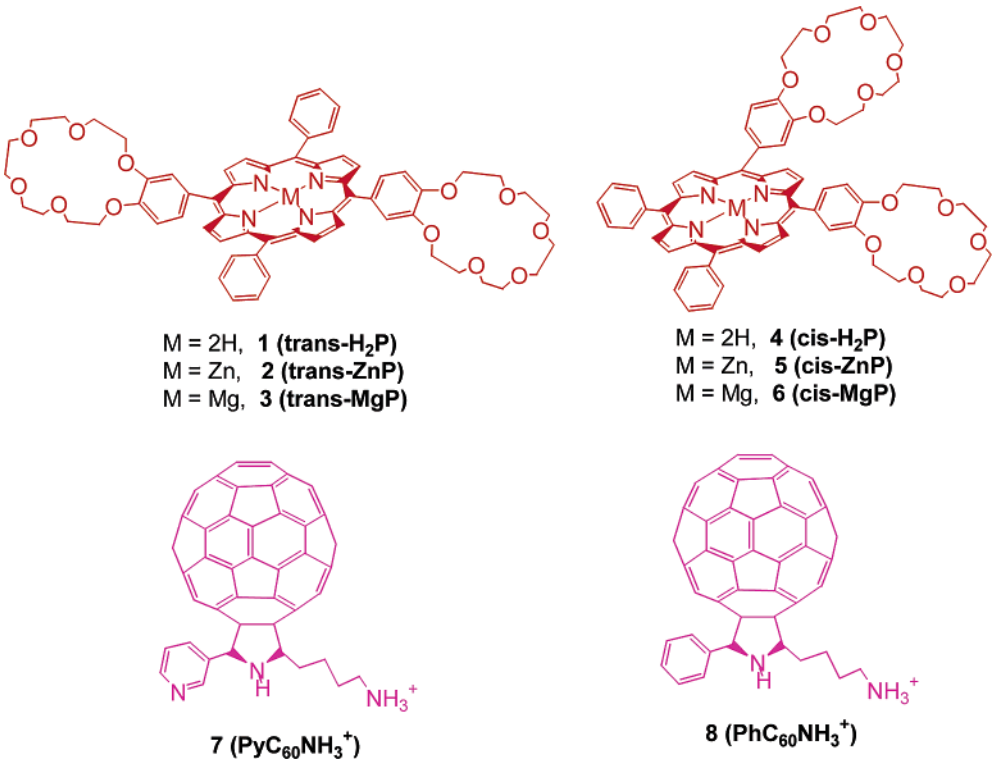

Here, we have extended our studies on building supramolecular conjugates using bis-18-crown-6 functionalized porphyrins, **1**−**6** (both cis and trans isomers), and fullerene functionalized to possess both a pyridine and an alkylammonium cation entity, **7** ($PyC_{60}NH_3^+$), or only an alkylammonium cation, **8** ($PhC_{60}NH_3^+$) (Scheme 1). The cis-isomer is functionalized at the 5,10 positions of the porphyrin ring while the trans-isomer is functionalized at the 5,15 positions of the porphyrin ring with the 18-crown-6 entities. Free-base, zinc, and magnesium metal porphyrins have been employed since they would form conjugates with different geometry and energetics in electron-transfer reactions. That is, the crown ether appended free-base porphyrins, **1** (*trans*-H_2P) or **4** (*cis*-H_2P), would bind to **7** ($PyC_{60}NH_3^+$) or **8** ($PhC_{60}NH_3^+$) through crown ether alkylammonium cation complexation with the possibility of additional $\pi-\pi$ interactions (Scheme 2a). This is also going to be the case when **8** ($PhC_{60}NH_3^+$) binds to any of the porphyrins, **1**−**6**. In the case of **2** (*trans*-ZnP) and **5** (*cis*-ZnP), addition of excess **7** ($PyC_{60}NH_3^+$) would result in a conjugate in which the pyridine of one of two fullerenes will be axial-coordinated to the zinc center and cation−crown ether complexation as shown in Scheme 2b. Interestingly, the magnesium porphyrins are expected to form bis-axial ligated complexes in addition to cation−crown ether complexation as shown in Scheme 2c,d. It may be mentioned here that when imidazole appended fullerene was utilized to form a self-assembled complex via the axial coordination approach, the magnesium porphyrin yielded only the pentacoordinated complex instead of the anticipated six-coordinated complex due to the large amount of fullerene derivative needed to accomplish the six-coordination.[14] By adopting the present "two-point" binding strategy, it is expected to yield such six-coordinated complexes due to the resulting higher stability of the complexes. Additionally, the oxidation potentials of the porphyrins generally follow the trend MgP < ZnP < H_2P.[15] This property, combined with the emission properties of the porphyrins, is expected to modulate the energetics of electron transfer. Systematic studies have been performed to visualize these trends and photoinduced electron transfer with steady-state and time-resolved spectroscopy performed on the supramolecular triads in the present study.

Results and Discussion

UV−Visible Spectral Studies and Ground-State Interactions. The optical absorption behavior of the cis and trans derivatized with bis-benzo-18-crown-6 appended metalloporphyrins was found to be similar to that of the corresponding pristine metallotetraphenylporphyrins.[16] That is, they exhibited an intense Soret band in the 415−430 nm range and less intense bands in the 500−700 nm region. No apparent absorption band in the 350−700 nm region corresponding to the crown ether entities was observed. Addition of **7** ($PyC_{60}NH_3^+$) or **8** ($PhC_{60}NH_3^+$) to a solution containing any of porphyrins **1**−**6** revealed spectral changes. However, the spectral changes were drastic when **7** ($PyC_{60}NH_3^+$) was titrated with **2** (*trans*-ZnP), **3** (*trans*-MgP), **5** (*cis*-ZnP), or **6** (*cis*-MgP) due to the axial coordination of the pyridine entity of **7** ($PyC_{60}NH_3^+$) binding to the metal center.[17] Typical spectral changes observed for **3** (*trans*-MgP) in the presence of increasing amounts **7** ($PyC_{60}NH_3^+$) are shown in Figure 1. Job's plots of continuous variation also confirmed the 1:2 molecular stoichiometry of the porphyrin:$(fullerene)_2$ supramolecular conjugates. It is important to note that the spectral changes observed for the magnesium porphyrin interacting with fullerene **7** ($PyC_{60}NH_3^+$) are that of the bis-pyridine coordinated species.[17c,d] This is in contrast to the earlier reported dyad involving magnesium tetraphenylporphyrin coordinating to imidazole appended fullerene where only a 1:1 complex was obtained.[14] In that study, the anticipated 1:2 complex could not be obtained due to the large amount of fullerene derivative needed to accomplish this task. This example nicely demonstrates the success of the "two-point" binding approach to accomplish structures that are otherwise difficult to form.

SCHEME 2: Structures of the Supramolecular Bis-fullerene−Porphyrin Conjugates According to the Metal Ion Present in the Porphyrin Cavity

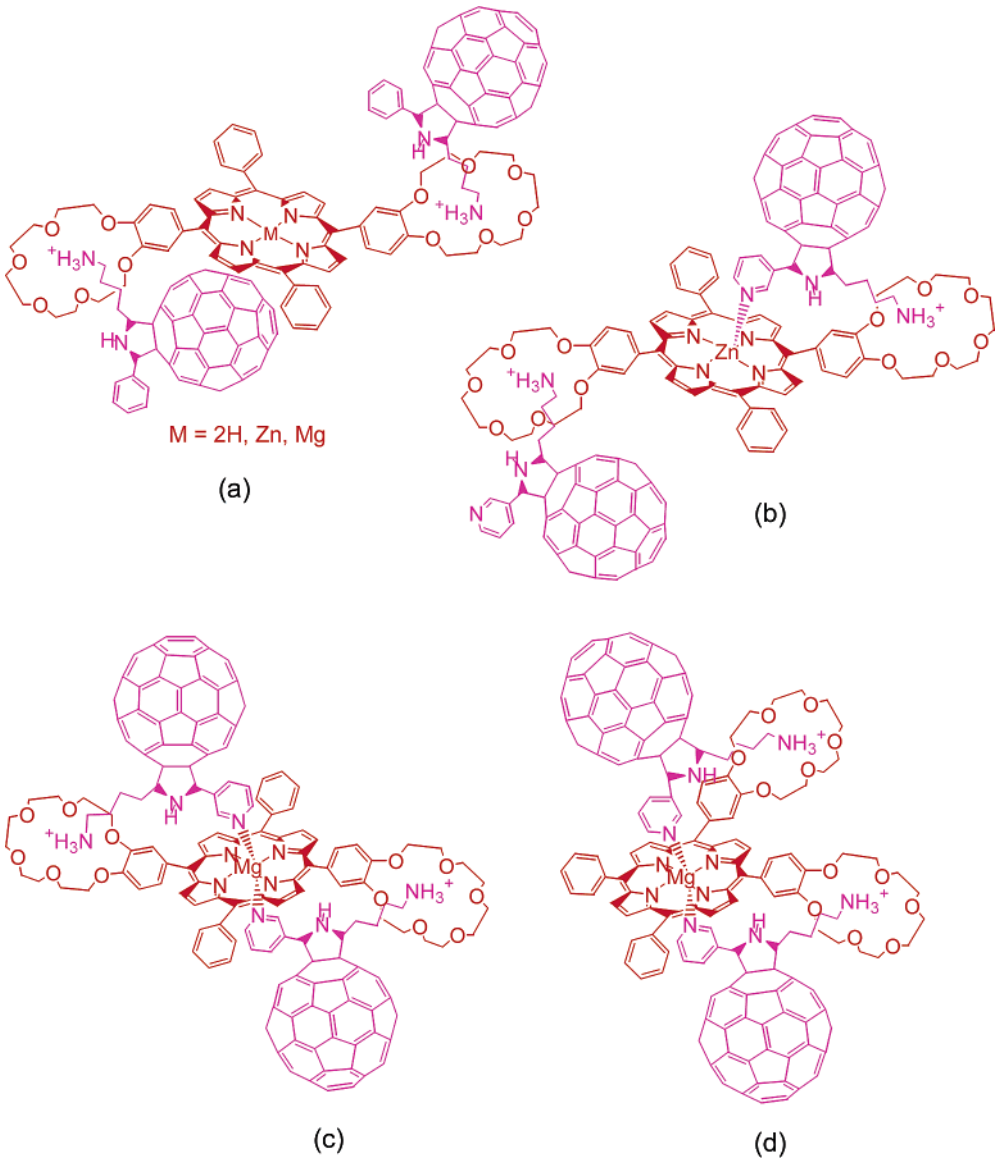

By using the spectral changes the binding constants, *K*, were evaluated with the Benesi−Hildebrand method.[18] However, we could not obtain reliable binding constants for conjugates formed by only crown ether−ammonium cation binding but with no axial coordination, that is, the conjugates formed from **1** (*trans*-H_2P) or **4** (*cis*-H_2P) with fullerene **8** ($PyC_{60}NH_3^+$), and all of the conjugates formed by fullerene **8** ($PhC_{60}NH_3^+$) having no pyridine functionality. This was due to the small spectral changes associated with the conjugate formation and appreciable absorbance of fullerene at the monitoring wavelength of porphyrin. As discussed in the subsequent section, by using fluorescence quenching data, it was possible to obtain reliable binding constants for all of the conjugates. Extending the absorption wavelength into the near-IR region (650−1000 nm) did not reveal new absorption bands corresponding to $\pi-\pi$ type interactions that would result in the case of conjugates shown in Scheme 2a,b. This is probably due to the extended free-base porphyrin absorption bands (up to 700 nm) into this wavelength region and weaker $\pi-\pi$ interactions in these conjugates.

Furthermore, ESI-mass spectral studies were performed to characterize the supramolecular conjugates. As shown in Figure 2, for a representative case of **3** (*trans*-MgP) interacting with **7** ($PyC_{60}NH_3^+$), a molecular ion peak corresponding to the 1:2 conjugate was observed. Very similar results were obtained for the other studied supramolecular conjugates. Recently, Solladiè et al.[19] also characterized 1:2 complexes of the type **1**:**8**$_2$ and **4**:**8**$_2$, that is, bis-crown ether appended free-base porphyrins and ammonium cation functionalized fullerene, and obtained similar ESI-mass spectral results.

Steady-State Fluorescence Studies. The singlet excited state quenching of cis and trans bis-crown ether appended porphyrins by functionalized fullerenes was investigated to obtain the binding constants of the self-assembled conjugates and the overall quenching behavior. The emission behavior of the bis-crown ether appended porphyrins was found to be similar to that of the corresponding pristine porphyrins with two emission bands. The position of the two crown ether entities had little or no effect on the wavelength maxima. The respective emission bands were located at 615 and 664 nm for the zinc porphyrins, 620 and 672 nm for the magnesium porphyrins, and 658 and 721 nm for the free-base porphyrins. Addition of **7** ($PyC_{60}NH_3^+$) or **8** ($PhC_{60}NH_3^+$) to a solution of any of the porphyrins, **1**−**6**, revealed fluorescence quenching. However, the quenching efficiency was found to be higher for **7** ($PyC_{60}NH_3^+$) binding

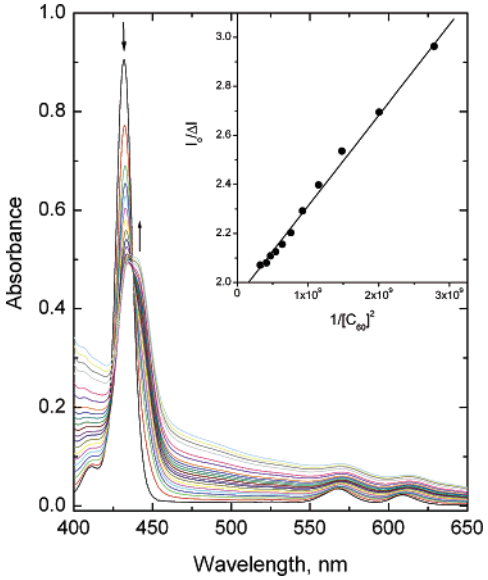

Figure 1. UV−visible spectral changes observed during the titration of **3** (*trans*-MgP) (1.1 μM) with **7** ($PyC_{60}NH_3^+$) (0.7 μM each addition) in benzonitrile. The figure inset shows a Benesi−Hildebrand plot constructed to obtain the binding constant with fluorescence data.

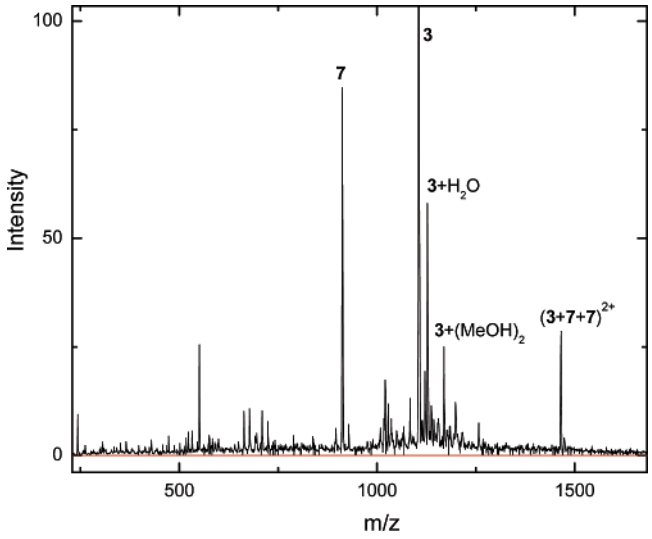

Figure 2. ESI-mass spectrum of the supramolecular triad formed by **3** (*trans*-MgP) and **7** ($PyC_{60}NH_3^+$) in dichloromethane.

to zinc or magnesium derivatives of the porphyrin derivatives due to two modes of binding. Representative emission changes of **3** (*trans*-MgP) on increasing addition of **7** ($PyC_{60}NH_3^+$) in benzonitrile are shown in Figure 3a. By using the emission data, the binding constants ($K_{app} = K_1K_2$) for the formation of self-assembled triads were obtained by constructing Benesi−Hildebrand plots[18] and the K_{app} values are listed in Table 1. It may be mentioned here that the K values for mono-18-crown-6 appended porphyrin binding to either **7** or **8** were in the range 10^4-10^5 M^{-1}.[13] A comparison of this K with K_{app} suggests that the magnitude of K_2 is close to that of K_1 in the investigated triads. The K_{app} values are higher for Zn or Mg porphyrins binding to **7** due to mono- or bis-axial coordination.

The Stern−Volmer plots for the fluorescence intensity quenching of the crown ether appended free-base porphyrins by **7** and **8** were constructed (Figure 3b). The calculated Stern−Volmer constant, K_{SV}, values were as high as 10^5 M^{-1}. On employing the excited state lifetime of the porphyrins, the fluorescence quenching rate constants, k_q, were evaluated to be

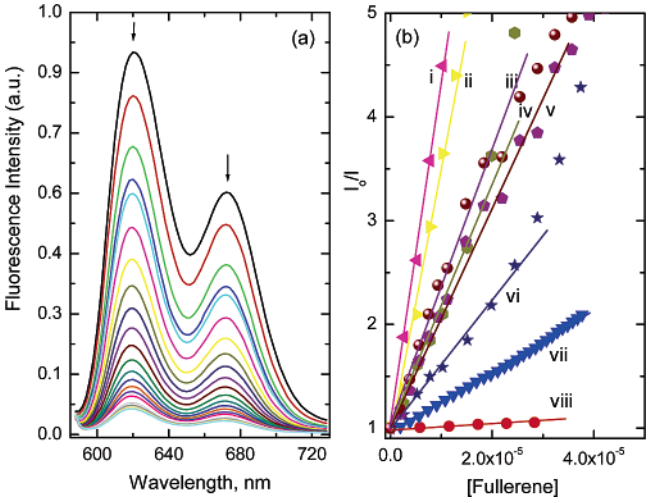

Figure 3. (a) Fluorescence spectral changes observed on increasing addition of **7** ($PyC_{60}NH_3^+$) (1.3 μM each addition) to a solution of porphyrin, **3** (*trans*-MgP, 1.4 μM) in benzonitrile. $\lambda_{ex} = 567.5$ nm. (b) Stern−Volmer plots for fluorescence quenching of (i) **5** (*cis*-ZnP) with **7** ($PyC_{60}NH_3^+$), (ii) **2** (*trans*-ZnP) with **7** ($PyC_{60}NH_3^+$), (iii) **1** (*trans*-H_2P) with **7** ($PyC_{60}NH_3^+$), (iv) **6** (*cis*-MgP) with **7** ($PyC_{60}NH_3^+$), (v) **4** (*cis*-H_2P) with **7** ($PyC_{60}NH_3^+$), (vi) **3** (*trans*-MgP) with **7** ($PyC_{60}NH_3^+$), (vii) mono-18-crown-6 appended free-base porphyrin with **7** ($PyC_{60}NH_3^+$), and (viii) mono-18-crown-6 appended free-base porphyrin with **8** ($PhC_{60}NH_3^+$) in benzonitrile.

over 10^{11} M^{-1} s^{-1}, which are up to 3 orders of magnitude higher than that expected for diffusion controlled-bimolecular quenching processes in the studied solvents ($\sim 5.0 \times 10^9$ M^{-1} s^{-1}) suggesting that the faster intrasupramolecular processes are responsible for the fluorescence quenching. The tendency of increasing in the K_{SV} values was in good agreement with those evaluated K values.

Semiempirical PM3 Calculations. To visualize the geometry of the bis-crown ether appended porphyrin−fullerene conjugates, PM3 calculations were performed. Representative examples of the space-filling model structures of the self-assembled conjugates are shown in Figure 4. It may be noted here that we could not perform higher level calculations due to the large size and flexible nature of these conjugates, although B3LYP/3-21G(*) calculations are expected to provide better geometry and electronic structure.[20] In all of the studied conjugates, the two crown ether entities formed stable complexes with the alkylammonium group of **7** ($PyC_{60}NH_3^+$) or **8** ($PhC_{60}NH_3^+$). However, different geometries were possible to achieve due to the additional pyridine−metal coordination. When **1** (*trans*-H_2P) and **3** (*cis*-H_2P) were self-assembled with 2 equiv of either of **7** ($PyC_{60}NH_3^+$) or **8** ($PhC_{60}NH_3^+$), a structure similar to that shown in Figure 4a was obtained. In these structures, one of the fullerene entities was close to the porphyrin π-system revealing some interactions while the second fullerene was far enough away to provide appreciable interactions with the porphyrin ring. This was also the case when the zinc and magnesium porphyrin derivatives were self-assembled with **8** ($PhC_{60}NH_3^+$) as shown in Figure 4b for the representative **2**:**8**$_2$ conjugate. When **7** ($PyC_{60}NH_3^+$) possessing both pyridine and alkylammonium cation functionalities was employed, only one pyridine−fullerene was coordinated to the zinc center, leaving the second pyridine−fullerene with only a crown ether−ammonium bond. Interestingly, when **3** (*trans*-MgP) and **6** (*cis*-MgP) were allowed to interact with **7** ($PyC_{60}NH_3^+$), bis-coordinated magnesium conjugates were obtained as shown in Figure 4c,d for the respective trans and cis isomers. These predictions are in agreement with the experimentally character-

TABLE 1: Electrochemical Half-Wave Redox Potentials ($E_{1/2}$ vs Fc/Fc$^+$) and Driving Forces for Forward and Reverse Electron Transfer for the Bis-crown Ether Appended Porphyrin−Fullerene Conjugates in the Presence of 0.1 M (n-Bu)$_4$NClO$_4$ in Benzonitrile

compound[a]	R_{CC}/Å	K_{app}[b]/M^{-2}	M$^{0/\bullet+}$/V	C$_{60}^{0/\bullet-}$/V	M$^{0/-}$/V	$-\Delta G_{CS}$/eV	$-\Delta G_{CR}$/eV
1 (*trans*-H$_2$P)			0.50		−1.65		
1:**8** (1:2)	9.1	1.16×10^{10}	0.52	−1.04	−1.65	0.44	1.51
4 (cis-H$_2$P)			0.50		−1.63		
4:**8** (1:2)	10.0	2.08×10^{10}	0.51	−1.04	−1.63	0.45	1.49
2 (*trans*-ZnP)			0.28		−1.83		
2:**8** (1:2)	11.1	2.50×10^{10}	0.27	−1.03	−1.85	0.80	1.24
2:**7** (1:2)	10.2	6.10×10^{10}	0.25	−1.03	−1.85	0.82	1.22
5 (*cis*-ZnP)			0.28		−1.83		
5:**8** (1:2)	10.0	4.27×10^{10}	0.25	−1.03	−1.85	0.82	1.22
5:**7** (1:2)	10.0	1.38×10^{11}	0.25	−1.03	−1.85	0.82	1.22
3 (*trans*-MgP)			0.18		−1.92		
3:**8** (1:2)	10.9	2.07×10^{10}	0.15	−1.02	−1.96	0.90	1.12
3:**7** (1:2)	10.5	2.50×10^{10}	0.12	−1.02	−1.96	0.93	1.09
6 (*cis*-MgP)			0.19		−1.91		
6:**8** (1:2)	10.0	2.30×10^{10}	0.16	−1.02	−1.95	0.90	1.12
6:**7** (1:2)	10.2	4.01×10^{10}	0.12	−1.02	−1.95	0.94	1.08

[a] See Scheme 1 for structures. [b] $K_{app} = K_1K_2$ (data from fluorescence quenching studies).

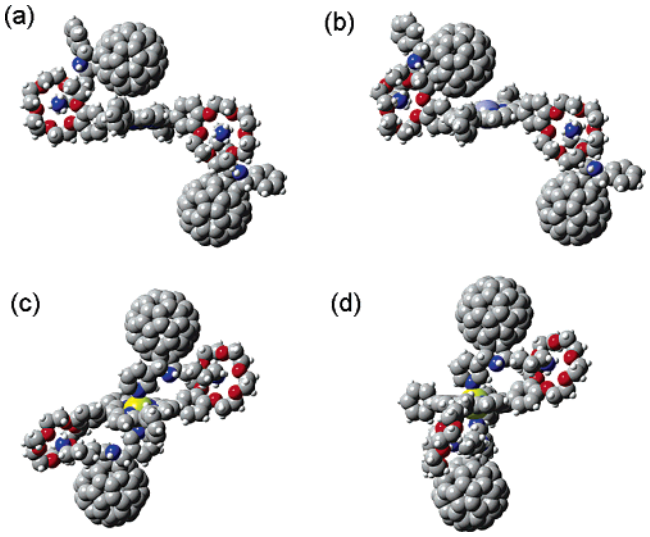

Figure 4. Semiempirical PM3 optimized space-filling model structures of (a) **1** (*trans*-H$_2$P):**8**$_2$ (PhC$_{60}$NH$_3^+$)$_2$, (b) **2** (*trans*-ZnP):**8**$_2$ (PhC$_{60}$NH$_3^+$)$_2$, (c) **3** (*trans*-MgP):**7**$_2$ (PyC$_{60}$NH$_3^+$)$_2$, and (d) **6** (*cis*-MgP):**7**$_2$ (PyC$_{60}$NH$_3^+$)$_2$ supramolecular conjugates.

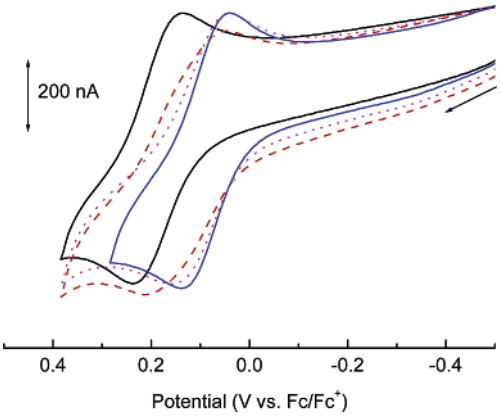

Figure 5. Cyclic voltammograms of **6** (solid dark line) on addition of 0.5 (red dash), 1.0 (magenta dot), and 2.0 equiv (solid blue) of **7** (PyC$_{60}$NH$_3^+$) in benzonitrile containing 0.1 M (n-Bu)$_4$NClO$_4$. Scan rate = 100 mV/s.

ized bis-pyridine-coordinated magnesium complex shown in Figure 4c,d. The center-to-center distance (R_{Ct-Ct}) between the metal and the center of the axially coordinated fullerene in these conjugates was about 10.5 Å, while the distance for the $\pi-\pi$ interacting porphyrin−fullerene was about 5.6 Å.

Electrochemical Studies. Cyclic voltammetric studies were performed to evaluate the redox potentials of the conjugates and to establish the free-energy changes for electron-transfer processes in the studied solvent. All of the investigated bis-crown ether appended porphyrins, **1**−**6**, revealed a one-electron oxidation process corresponding to the formation of MP$^{\bullet+}$ (M = 2H, Zn, or Mg), and two one-electron reductions corresponding to the formation of MP$^{\bullet-}$ and MP^{2-}, respectively. Extending the potential window beyond the first oxidation process resulted in a large anodic wave, perhaps due to the oxidation of the appended crown−ether entities.[21] The first oxidation potential followed the trend MgP < ZnP < H$_2$P, while an opposite trend was observed for the first reduction process. Fullerenes **7** (PyC$_{60}$NH$_3^+$) and **8** (PhC$_{60}$NH$_3^+$) upon binding to the porphyrins revealed no significant changes in their reduction potentials. However, depending upon the mode of binding the oxidation potentials of the porphyrins revealed cathodic shifts, as listed in Table 1. Maximum potential shifts were observed for magnesium porphyrins binding to PyC$_{60}$NH$_3^+$ (up to 70 mV), as a result of the axial coordination. To verify whether the resulting shifts are upon formation of 1:1 or 1:2 complexation, titrations were carried out by stepwise addition of **7** (0.5 equiv each addition) to the benzonitrile solution containing MgP. As shown in Figure 5, the anodic shift was complete with only one equivalent addition of **7** (PyC$_{60}$NH$_3^+$). The second equivalent addition of fullerene did not result in any additional potential shifts. On addition of **8** (PhC$_{60}$NH$_3^+$) having no axial coordinating ability, the observed potential shifts were less than 30 mV.

The driving forces for charge recombination ($-\Delta G_{CR}$) and charge separation ($-\Delta G_{CS}$) were calculated according to eqs 1 and 2, using the electrochemical redox data:[22]

$$-\Delta G_{CR} = E_{ox} - E_{red} - \Delta G_s \quad (1)$$

$$-\Delta G_{CS} = E_{0,0} - (-\Delta G_{CR}) \quad (2)$$

where E_{ox} is the first oxidation potential of the porphyrin (MP$^{0/\bullet+}$), E_{red} is the first reduction potential of the fullerene (C$_{60}^{0/\bullet-}$), $\Delta E_{0,0}$ is the energy of the 0−0 transition between the lowest excited state and the ground state of the porphyrin evaluated from the fluorescence emission peaks, and ΔG_s refers to the static energy, calculated by using the "Dielectric Continuum Model"[22] according to eq 3.

$$\Delta G_s = e^2/(4\pi\epsilon_0\epsilon_s R_{Ct-Ct}) \quad (3)$$

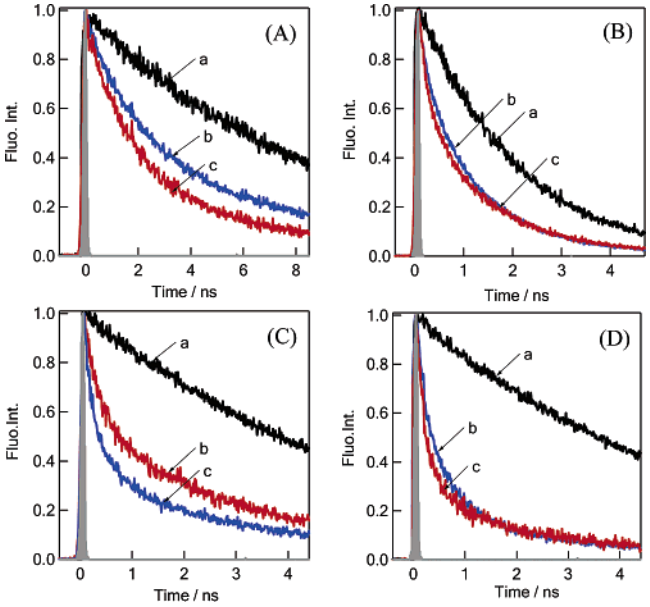

Figure 6. Fluorescence decays for the following: (A) (a) **1** (*trans*-H_2P) (0.07 mM), (b) **1** (*trans*-H_2P) (0.07 mM) + **8** ($PhC_{60}NH_3^+$) (0.07 mM), and (c) **1** (*trans*-H_2P) (0.07 mM) + **8** ($PhC_{60}NH_3^+$) (0.14 mM); (B) (a) **2** (*trans*-ZnP) (0.07 mM), (b) **2** (*trans*-ZnP) (0.07 mM) + **8** ($PhC_{60}NH_3^+$) (0.07 mM), and (c) **8** ($PhC_{60}NH_3^+$) (0.14 mM); (C) (a) **3** (*trans*-MgP) (0.07 mM), (b) **3** (*trans*-MgP) (0.07 mM) + **7** (0.07 mM), and (c) **3** (*trans*-MgP) (0.07 mM) + **7** ($PyC_{60}NH_3^+$) (0.14 mM); (D) (a) **6** (*cis*-MgP) (0.07 mM), (b) **6** (*cis*-MgP) (0.07 mM) + **7**($PyC_{60}NH_3^+$) (0.07 mM), and (c) **6** (*cis*-MgP) (0.07 mM) + **7** ($PyC_{60}NH_3^+$) (0.14 mM). The porphyrins were excited at 400 nm in benzonitrile solvent.

The symbols ϵ_0 and ϵ_s represent the vacuum permittivity and the dielectric constant of the solvent benzonitrile, respectively. Values of R_{Ct-Ct} were based on the computed structures shown in Figure 4 and discussed in the previous section.

The calculated free-energy changes in Table 1 reveal that the charge separation from the singlet excited porphyrin to fullerene in these dyads is exothermic and follows the order H_2P < ZnP < MgP of a given porphyrin derivative. These results predict the occurrence of rapid charge separation in these supramolecular dyads since the ΔG_{CS} values are almost on the top region of the Marcus parabola. On the other hand, the charge recombination in the charge-separated state ($MP^{\bullet+}$:$C_{60}^{\bullet-}$) of the supramolecular conjugates is predicted to be a slower process since the highly exothermic ΔG_{CR} values lie on the inverted region of the Marcus parabola.

Picosecond Time-Resolved Emission. The time-resolved emission studies of the self-assembled conjugates tracked those of steady-state quenching measurements. Figure 6 shows the emission decay profiles of the representative bis-crown ether appended porphyrins in the absence and presence of fullerene derivatives. The bis-crown appended porphyrins revealed mono-exponential decays with lifetimes of 9.0, 1.9, and 5.1 ns respectively for H_2P, ZnP, and MgP. The appended crown ether moieties had a small quenching effect on the lifetimes of the singlet excited porphyrins. Addition of fullerene to the bis-crown ether appended porphyrins caused rapid fluorescence decay in addition to a slow decaying tail as shown in curves b (for one equivalent addition) and c (for two equivalent additions) in Figure 6A−D. The porphyrin emission decay in the dyads could be fitted satisfactorily by a biexponential decay curve, the lifetimes (τ_f) of which are summarized in Table 2. The short lifetimes of MP were predominantly due to charge separation within the supramolecular conjugates ($(\tau_f)_{complex}$), whereas the long lifetime components are attributed to the uncomplexed porphyrin emission.

The charge-separated rates (k^S_{CS}) and quantum yields (Φ^S_{CS}) were evaluated from the $(\tau_f)_{complex}$ values according to eqs 4 and 5, a procedure commonly adopted for intramolecular electron-transfer process.[23]

$$k^S_{CS} = (1/\tau_f)_{complex} - (1/\tau_f)_{MP} \quad (4)$$

$$\Phi^S_{CS} = [(1/\tau_f)_{complex} - (1/\tau_f)_{MP}]/(1/\tau_f)_{complex} \quad (5)$$

As listed in Table 2, higher values of k^S_{CS} and Φ^S_{CS} were obtained for all of the dyads indicating the occurrence of efficient charge separation irrespective of the location of the crown ether entities on the porphyrin macrocycle and the type of employed fullerene derivative for conjugate formation. However, specific trends could be observed from these kinetic results. These include the following: (i) For a given porphyrin derivative interacting with **8** ($PhC_{60}NH_3^+$), the k_{CS} and Φ_{CS} followed the trend H_2P < ZnP < MgP. That is, they tracked the free-energy values given in Table 1. (ii) The k_{CS} and Φ_{CS} values are higher for ZnP and MgP interacting with **7** ($PyC_{60}NH_3^+$) due to the two-point binding and the resulting structural rigidity. (iii) The k_{CS} and Φ_{CS} values are higher for the cis bis-crown compared to the trans bis-crown derivative porphyrins. This trend agrees readily with the binding and steady-state quenching observations (Figure 3b). (iv) The k_{CS} and Φ_{CS} values are higher for **2**:$\mathbf{7}_2$, **2**:$\mathbf{8}_2$, **5**:$\mathbf{7}_2$, and **5**:$\mathbf{8}_2$ compared to the earlier reported 1:1 mono-crown ether appended zinc porphyrin: fullerene dyads involving **7** ($PyC_{60}NH_3^+$) and **8** ($PhC_{60}NH_3^+$). This observation clearly indicates that employing a higher number of acceptor entities improves the charge-separation efficiency. Furthermore, nanosecond transient absorption spectral studies were also performed to characterize the charge-separated states and evaluate the kinetic results of the charge-recombination process.

Nanosecond Transient Absorption Studies. The nanosecond transient spectra recorded after 532 or 550 nm laser irradiation of the bis-crown ether appended porphyrins, **1**−**6**, revealed absorption peaks corresponding to their excited triplet state of porphyrins.[24] Fullerenes **7** ($PyC_{60}NH_3^+$) and **8** ($PhC_{60}NH_3^+$) showed a band around 700 nm corresponding to their excited triplet states.[25,26] Figure 7 shows the transient absorption spectra of the representative conjugates. In these spectra, in addition to the peaks corresponding to the triplet excited free-base porphyrin and fullerene, a peak around 1020 nm corresponding to the formation of fullerene anion radical was observed. The absorption band of the radical cation of the porphyrins, expected to appear in the 600−700 nm region as a counterpart of the fullerene anion radical, was difficult to observe due to the strong emission of the porphyrins in this wavelength region. However, the spectral features of fullerene anion radical provided an experimental proof for the generation of the charge-separated state ($MP^{\bullet+}$:$C_{60}^{\bullet-}$) as a consequence of fluorescence quenching.

As shown in the inset of Figure 7A−F, the time profile of the $C_{60}^{\bullet-}$ transient band at 1020 nm was monitored for obtaining kinetic information for the charge recombination process. In each time profile, an initial decay followed by slow decay was observed. It may be mentioned here that the initial time profiles of these peaks for all of the studied conjugates followed the first-order decay kinetics, once again suggesting the occurrence of the intramolecular charge-recombination process of the radical ion pair. The lifetimes of the radial ion pairs, τ_{RIP}, evaluated as the reciprocal of the charge-recombination rates (k_{CR}), are listed

TABLE 2: Fluorescence Lifetimes (τ_f), Charge-Separation Rate Constants (k^S_{CS}),[a] Charge-Separation Quantum Yields (Φ^S_{CS}),[a] Charge-recombination Rate Constants (k_{CR}), and Lifetime of the Radical Ion Pairs of the Investigated Bis-crown Ether Appended Porphyrin−C_{60} Conjugates in Benzonitrile

compound[a]	τ_f/ps	k^S_{CS}/s^{-1}	Φ^S_{CS}	$k_{CR}{}^b/s^{-1}$	$\tau_{RIP}{}^b$/ns
1:**8** (1:1)	1860 (55%), 7500 (45%)	4.2×10^8	0.79	4.61×10^6	217
1:**8** (1:2)	1670 (68%), 6400 (32%)	4.9×10^8	0.81	6.86×10^6	146
4:**8** (1:1)	1000 (58%), 7800 (42%)	8.9×10^8	0.89	8.28×10^6	121
4:**8** (1:2)	970 (66%), 6100 (34%)	9.2×10^8	0.89	1.06×10^7	94
2:**8** (1:1)	366 (55%), 1500 (45%)	2.2×10^9	0.81	4.30×10^6	233
2:**8** (1:2)	265 (60%), 1400 (40%)	3.3×10^9	0.86	8.30×10^6	121
2:**7** (1:1)	252 (60%), 1550 (40%)	3.4×10^9	0.87	6.10×10^6	164
2:**7** (1:2)	220 (65%), 1450 (35%)	4.0×10^9	0.88	9.20×10^6	109
5:**8** (1:1)	297 (56%), 1600 (44%)	2.8×10^9	0.84	5.33×10^6	188
5:**8** (1:2)	235 (60%), 1500 (40%)	3.7×10^9	0.88	7.37×10^6	137
5:**7** (1:1)	209 (58%), 1500 (42%)	4.3×10^9	0.89	7.00×10^6	143
5:**7** (1:2)	198 (69%), 1450 (31%)	4.5×10^9	0.90	9.60×10^6	104
3:**8** (1:1)	320 (67%), 3500 (33%)	2.9×10^9	0.94	7.50×10^6	133
3:**8** (1:2)	280 (72%), 2600 (28%)	3.4×10^9	0.95	9.50×10^6	105
3:**7** (1:1)	315 (60%), 3200 (40%)	3.0×10^9	0.94	1.45×10^7	69
3:**7** (1:2)	225 (68%), 2600 (32%)	4.3×10^9	0.96	2.20×10^7	46
6:**8** (1:1)	305 (60%), 2720 (40%)	3.1×10^9	0.94	6.54×10^6	153
6:**8** (1:2)	250 (62%), 2900 (38%)	3.8×10^9	0.95	9.04×10^6	111
6:**7** (1:1)	240 (71%), 2700 (29%)	3.9×10^9	0.95	8.35×10^6	120
6:**7** (1:2)	200 (74%), 2300 (26%)	4.8×10^9	0.96	1.20×10^7	83

[a] The single exponential τ values of free-base, zinc, and magnesium porphyrins were 9000, 1900, and 5100 ps, respectively. [b] See text for details

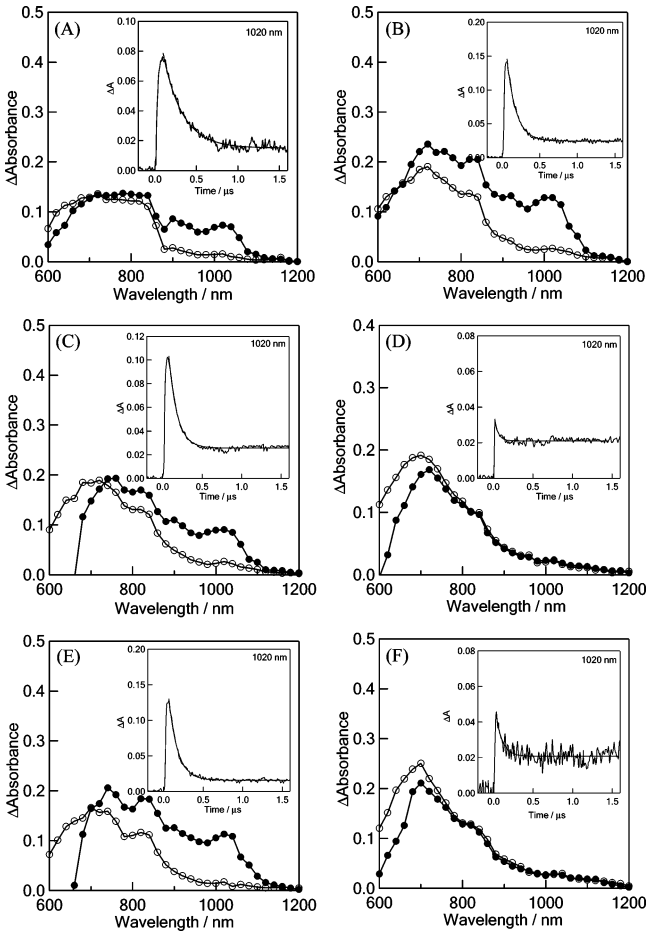

Figure 7. Nanosecond transient absorption spectra of the following: (A) **2** (*trans*-ZnP) (0.1 mM) in the presence of **8** ($PhC_{60}NH_3^+$) (0.1 mM); (B) **2** (*trans*-ZnP) (0.1 mM) in the presence of **8** ($PhC_{60}NH_3^+$) (0.2 mM); (C) **3** (*trans*-MgP) (0.1 mM) in the presence of **8** ($PhC_{60}NH_3^+$) (0.2 mM); (D) **3** (*trans*-MgP) (0.1 mM) in the presence of **7** ($PyC_{60}NH_3^+$) (0.2 mM); (E) **6** (*cis*-MgP) (0.1 mM) in the presence of **8** ($PhC_{60}NH_3^+$) (0.2 mM); (F) **6** (*cis*-MgP) (0.1 mM) in the presence of **7** ($PyC_{60}NH_3^+$) (0.2 mM). All the spectra were recorded at 100 (●) and 1000 ns (○) in benzonitrile after the 550 nm laser irradiation. The figure insets show the time profiles of the transient bands at the indicated wavelengths.

in Table 2. The calculated k_{CR} values were 2−3 orders of magnitude smaller than the k_{CS} values, suggesting the occurrence of the charge recombination process in the Marcus inverted region. The τ_{RIP} values range between 46 and 233 ns indicating charge stabilization in the studied conjugates and higher values were observed for conjugates formed by **8** ($PhC_{60}NH_3^+$). No specific trend with respect to different porphyrins could be observed from the present results. As for the slow decay part, a portion may be attributed to the absorption tail of the triplet states of the porphyrin and fullerene entities with lifetimes on the order of 50−100 μs in the long time-scale measurements. Some part of the decay was prolonged beyond the triplet state lifetimes suggesting the occurrence of intermolecular electron transfer between uncomplexed components via the triplet states, since the slow rise until ca. 50 μs was observed with longer lifetimes in the order of 300−500 μs.

Summary

Free-base, zinc, and magnesium porphyrins possessing two 18-crown-6 entities at the cis or trans positions of the porphyrin ring have been synthesized and characterized. These porphyrins formed self-assembled conjugates with fullerenes functionalized with alkylammonium and/or pyridine functionalized fullerenes with well-defined structures. "Two-point" binding was observed in the case of fullerenes functionalized with pyridine and alkylammonium groups with metalloporphyrins. A 1:2 stoichiometry of the supramolecular porphyrin:fullerene conjugates was deduced from the optical absorption and emission, electron spray ionization mass, electrochemistry, and semiempirical PM3 calculations. In general, the k_{CS} and Φ_{CS} values were higher for the present 1:2 porphyrin:fullerene conjugates as compared to the earlier reported 1:1 porphyrin:fullerene conjugates using the same binding methodologies. The experimentally determined k_{CR} values from nanosecond transient absorption studies were 2−3 orders of magnitude smaller than the k_{CS} values, suggesting the occurrence of the charge recombination process in the Marcus inverted region, and charge stabilization in the studied conjugates.

Experimental Section

Chemicals. Fullerene C_{60} was from SES Research, Houston, TX. The syntheses and characterization of **7** ($PyC_{60}NH_3^+$) and

8 ($PhC_{60}NH_3^+$) are given elsewhere[13] and were freshly purified over silica gel column prior to the spectral studies. All the chromatographic materials and solvents were procured from Fisher Scientific and were used as received. Tetra-*n*-butylammonium perchlorate, $(n\text{-}C_4H_9)_4NClO_4$, was from Fluka Chemicals. All other chemicals utilized in the synthesis were from Aldrich Chemicals (Milwaukee, WI) and were used as received.

Synthesis of 4′-Formylbenzo[18-crown-6]. The title compound was synthesized by two different procedures.

Method A: A mixture of 3,4-dihydroxybenzaldehyde (1 g, 7.24 mmol) and K_2CO_3 (5 g, 36.2 mmol) was taken in DMF (10 mL). Pentaethyleneglycol di-*p*-toluenesulfonate (4.354 g, 3.483 mL, 7.964 mmol) was added to it with stirring and the solution was refluxed under argon for 18 h. The cooled mixture was acidified with dilute HCl and then filtered. The filtrate was evaporated to dryness and the residue was extracted with $CHCl_3$ 3 or 4 times. The extract was evaporated to yield a viscous oil that was purified over silica gel column initially with toluene: $CHCl_3$ (40:60 v/v) and finally with $CHCl_3$:MeOH (98:2 v/v). On trituration with diethyl ether a white fibrous product was obtained, which on crystallization from ethanol gave the desired product. Yield: 1.8 g (75%).

Method B: Benzo-18-crown-6 (2.52 g, 8.07 mmol) and hexamethylenetetramine (1.2 g, 8.5 mmol) were mixed with trifluoroacetic acid (6.1 mL, 78.6 mmol) and the reaction mixture was heated to 100 °C under N_2 for 24 h.[27] The resulting dark red mixture was cooled to 5 °C, mixed with ice, and stirred for 1 h. The product was extracted with chloroform and the organic layer was dried over Na_2SO_4. The organic extract was evaporated to yield a viscous oil that was purified through column chromatography over silica gel, using $CHCl_3$:MeOH (98:2 v/v) as eluent. Evaporation of the solvent yielded pale-yellow oil, which upon trituration with diethyl ether and refrigeration gave the desired product as a white solid. Yield 1.64 g (60%). ^{1}H NMR (400 MHz, $CDCl_3$, 25 C, TMS) δ (ppm) 9.84 (s, 1H), 7.44 (dd, 1H, phenyl *H*), 7.39 (d, 1H, phenyl *H*), 6.95 (d, 1H, phenyl *H*), 4.28−4.18 (m, 4H, crownethylene *H*), 4.02−3.90 (m, 4H, crownethylene *H*), 3.82−3.71 (m, 8H, crownethylene *H*), 3.69 (s, 4H, crownethylene *H*).

H_2-*trans*- and *cis*-Di(benzo[18]crown-6)diphenylporphyrins, 1 and 4. A mixture of 4′-formylbenzo[18]crown-6 (**1**) (600 mg, 1.763 mmol), benzaldehyde (179.23 μL, 187.11 mg, 1.763 mmol), and pyrrole (244 μL, 236.24 mg, 3.53 mmol) was refluxed in propionic acid (200 mL) for 3.5 h. The propionic acid was removed under reduced pressure. Column chromatography on neutral alumina with $CHCl_3$ as eluent gave a mixture of five porphyrins including **1** and **4**. Subsequent column chromatography on neutral alumina yielded **1** (hexanes: $CHCl_3$ = 30:70 v/v) and **4** (hexanes:$CHCl_3$ = 20:80 v/v) as third and fourth fractions, respectively. **H_2-5,15-Di(benzo[18]-crown-6)-10,20-diphenylporphyrin (*trans*-1):** Yield 13.7 mg (∼1%). ^{1}H NMR (400 MHz, $CDCl_3$, 25 °C, TMS) δ (ppm) 8.87 (dd, 8 H, β-pyrrolic *H*), 8.22(d, 4 H, *o*-phenyl *H*), 7.82−7.69 (m, 10 H, *m*,*p*-phenyl *H* (6 H) and benzocrownphenyl *H*(4 H)), 7.21 (d, 2 H, benzocrownphenyl *H*), 4.48−4.42 (m, 4 H, crownethylene *H*), 4.31−4.26 (m, 4 H, crownethylene *H*), 4.14−4.08 (m, 4 H, crownethylene *H*), 3.99−3.88 (m, 8 H, crownethylene *H*), 3.85−3.73 (m, 20 H, crownethylene *H*), −2.79 (br s, 2 H, imino *H*). UV/vis (toluene) λ_{max} (nm) 426, 519, 554.5, 592.5, 651 nm. **H_2-5,10-di-(benzo-[18]-crown-6)-15, 20-diphenylporphyrin (*cis*-4):** Yield 24.9 mg (∼1.3%). ^{1}H NMR (400 MHz, $CDCl_3$, 25 °C, TMS) δ (ppm) 8.94−8.82 (m, 8 H, β-pyrrolic *H*), 8.25−8.18 (m, 4 H, *o*-phenyl *H*), 7.81−7.68 (m, 10 H, *m*,*p*-phenyl *H* (6 H) and benzocrownphenyl *H*(4 H)), 7.19 (d, 2 H, benzocrownphenyl *H*), 4.46−4.40 (m, 4 H, crownethylene *H*), 4.32−4.26 (m, 4 H, crownethylene *H*), 4.13−4.07 (m, 4 H, crownethylene *H*), 3.99−3.87 (m, 8 H, crownethylene *H*), 3.85−3.73 (m, 20 H, crownethylene *H*), −2.79 (br s, 2 H, imino *H*). UV/vis (toluene) λ_{max} 425.5, 518.5, 554.5, 592.5, 651 nm.

5,15-Di(benzo[18]crown-6)-10,20-diphenylporphyrinatozinc-(II) (*trans*-2). The free-base porphyrin **1** (10 mg, 0.009 mmol) was dissolved in $CHCl_3$ (10 mL), a saturated solution of zinc acetate in methanol was added to the solution, and the resulting mixture was refluxed for 2 h. The course of the reaction was followed spectrophotometrically by monitoring the disappearance of the 516 nm band of **2**. At the end, the reaction mixture was washed with water and dried over anhydrous Na_2SO_4. Chromatography on neutral alumina column by using hexanes: $CHCl_3$ (30:70 v/v) gave the title compound. Yield 9.3 mg (∼90%). ^{1}H NMR (400 MHz, $CDCl_3$, 25 °C, TMS) δ (ppm) 8.96 (dd, 8 H, β-pyrrolic *H*), 8.22 (d, 4 H, *o*-phenyl *H*), 7.80−7.68 (m, 10 H, *m*,*p*-phenyl *H* (6 H) and benzocrownphenyl *H*(4 H)), 7.17 (d, 2 H, benzocrownphenyl *H*), 4.34−4.29 (m, 4 H, crownethylene *H*), 4.18−4.11 (m, 4 H, crownethylene *H*), 3.92−3.87 (m, 4 H, crownethylene *H*), 3.77−3.56 (m, 28 H, crownethylene *H*). UV/vis (toluene) λ_{max} 432, 560, 603 nm. ESI mass in CH_2Cl_2 *m*/*z* (%) calcd 1146.62, found 1146.2 (85) $[M]^+$, 1144.2 (100).

10-Di(benzo[18]crown-6)-15, 20-diphenylporphyrinatozinc-(II) (*cis*-5). This compound was prepared from porphyrin **3** (10 mg, 0.009 mmol) according to the procedure outlined above for **4**. Yield:9.3 mg (∼90%). ^{1}H NMR (400 MHz, $CDCl_3$, 25 °C, TMS) δ (ppm) 8.99−8.90 (m, 8 H, β-pyrrolic *H*), 8.25−8.18 (m, 4 H, *o*-phenyl *H*), 7.79−7.65 (m, 10 H, *m*,*p*-phenyl *H* (6 H) and benzocrownphenyl *H*(4 H)), 7.12−7.06 (m, 2 H, benzocrownphenyl *H*), 4.19−4.12 (m, 4 H, crownethylene *H*), 4.07−3.98 (m, 4 H, crownethylene *H*), 3.71−3.61 (m, 4 H, crownethylene *H*), 3.60−3.38 (m, 28 H, crownethylene *H*). UV/vis (toluene) λ_{max} 431.5, 560.5, 602.5 nm. ESI mass in CH_2Cl_2 *m*/*z* (%) calcd 1146.62, found 1146.3 (100) $[M]^+$, 1177.2 (92) $[M + MeOH]^+$.

5,15-Di(benzo[18]crown-6)-10, 20-diphenylporphyrinato-magnesium(II) (*trans*-3). This compound was prepared according to a general procedure developed by Lindsey and Woodford[28] for Mg porphyrin synthesis. A sample of 10 mg (0.00925 mmol) of **2** was dissolved in 10 mL of CH_2Cl_2. Then 0.026 mL (18.72 mg, 0.19 mmol) of triethylamine was added followed by 23.9 mg (0.093 mmol) of $MgBr_2{\cdot}O(Et)_2$. The mixture was stirred for 20 min at room temperature. The course of the reaction was monitored by absorption spectroscopy. The mixture was diluted with 20 mL of CH_2Cl_2, washed with 5% $NaHCO_3$, and dried over anhydrous Na_2SO_4, then the filtrate was evaporated. Chromatography on neutral alumina column with $CHCl_3$ as eluent yielded residual **2**. Elution with $CHCl_3$: methanol (98:2 v/v) yielded a greenish purple fraction of the desired compound. Yield: 8 mg (∼80%). ^{1}H NMR (400 MHz, $CDCl_3$, 25 °C, TMS) δ (ppm) 8.96−8.85 (m, 8 H, β-pyrrolic *H*), 8.25−8.12 (m, 4 H, *o*-phenyl *H*), 7.75−7.56 (m, 10 H, *m*,*p*-phenyl *H* (6 H) and benzocrownphenyl *H*(4 H)), 6.98−6.88 (m, 2 H, benzocrownphenyl *H*), 3.91−3.33 (m, 8 H, crownethylene *H*), 3.28−2.53 (m, 32 H, crownethylene *H*). UV/vis (toluene) λ_{max} 432, 568, 609 nm. ESI mass in CH_2Cl_2 *m*/*z* (%) calcd 1105.54, found 1105.54 (60) $[M]^+$, 1127.8 (100) $[M + Na]^+$.

5,10-Di(benzo[18]crown-6)-15, 20-diphenylporphyrinato-magnesium(II) (*cis*-6). This compound was prepared from porphyrin **3** (10 mg, 0.009 mmol) according to the procedure outlined above for **6**. Yield 8 mg (∼80%). ^{1}H NMR (400 MHz,

$CDCl_3$, 25 °C, TMS) δ (ppm) 9.04−8.84 (m, 8 H, β-pyrrolic *H*), 8.28−8.15 (m, 4 H, *o*-phenyl *H*), 7.80−7.53 (m, 10 H, *m,p*-phenyl *H* (6 H) and benzocrownphenyl *H*(4 H)), 6.93−6.83 (m, 2 H, benzocrownphenyl *H*), 3.85−3.33 (m, 8 H, crownethylene *H*), 3.25−2.44 (m, 32 H, crownethylene *H*). UV/vis (toluene) λ_{max} 432, 568, 609 nm. ESI mass in CH_2Cl_2 *m/z* (%) calcd 1105.54, found 1105.6 (100) $[M]^+$.

Instrumentation. The UV−visible spectral measurements were carried out with a Shimadzu UV-1650PC spectrophotometer. The fluorescence emission was monitored by using either Spex Fluorolog-tau or Varian Cary Eclipse spectrometers. The right angle method was utilized. Cyclic voltammograms were recorded on a EG&G Model 263A potentiostat using a three-electrode system. A platinum or glassy carbon electrode was used as the working electrode. A platinum wire served as the counter electrode and a Ag/AgCl electrode was used as the reference electrode. A ferrocene/ferrocenium redox couple was used as an internal standard. All the solutions were purged prior to electrochemical and spectral measurements with argon gas. The computational calculations were performed by using semiempirical PM3 methods with the GAUSSIAN 03 software package[29] on high-speed computers.

Time-Resolved Emission and Transient Absorption Measurements. The picosecond time-resolved fluorescence spectra were measured by using an argon-ion pumped Ti:sapphire laser (Tsunami; pulse width = 2 ps) and a streak scope (Hamamatsu Photonics; response time = 10 ps). The details of the experimental setup are described elsewhere.[30] Nanosecond transient absorption spectra in the NIR region were measured by means of laser-flash photolysis; 532 or 550 nm light from a Nd:YAG laser (pulse width = 6 ns) was used as the exciting source and a Ge-avalanche-photodiode module was used for detecting the monitoring light from a pulsed Xe-lamp for shorter time scale measurements than 5 μs. For longer time scale measurements than 5 μs, the InGaAs photodiode detector was used to detect the monitoring light from a continuous Xe lamp.

Acknowledgment. The authors are thankful to Travis Cooper for recording the ESI-mass spectra. This work is supported by the National Science Foundation (Grant no. 0453464 to F.D.), the donors of the Petroleum Research Fund, administered by the American Chemical Society, and Grants-in-Aid for Scientific Research on Primary Area (417) from the Ministry of Education, Science, Sport and Culture of Japan (to O.I. add Y.A.).

References and Notes

(1) (a) Guldi, D. M. *Chem. Commun.* **2000**, 321. (b) Guldi, D. M.; Prato, M. *Acc. Chem. Res.* **2000**, *33*, 695. (c) Guldi, D. M. *Chem. Soc. Rev*. **2002**, *31*, 22. (d) Meijer, M. E.; van Klink, G. P. M.; van Koten, G. *Coord. Chem. Rev*. **2002**, *230*, 141. (e) El-Khouly, M. E.; Ito, O.; Smith, P. M.; D'Souza, F. *J. Photochem. Photobiol. C. Rev*. **2004**, *5*, 79. (f) Imahori, H.; Fukuzumi, S. *Adv. Funct. Mater*. **2004**, *14*, 525. (g) D'Souza, F.; Ito, O. *Coord. Chem. Rev*. **2005**, *249*, 1410. (h) Sanchez, L.; Martin, N.; Guldi, D. M. *Angew. Chem., Int. Ed*. **2005**, *44*, 5374.

(2) (a) Balzani V.; Scandola, F. *Supramolecular Chemistry*; Ellis Horwood, New York, 1991. (b) Schlicke, B.; De Cola, L.; Belser, P.; Balzani, V. *Coord. Chem. Rev*. **2000**, *208*, 267.

(3) *Supramolecular Chemistry*; Atwood, J. L., Davies, J. E. D., MacNicol, D. D., Vögtle, F., Reinhoudt, D. N., Eds.; Pergamon: Oxford, 1996; Vol. 10, pp 171−185.

(4) Connolly, J. S.; Bolton, J. R. In *Photoinduced Electron Transfer*; Fox, M. A., Chanon, M., Eds.; Elsevier: Amsterdam, The Netherlands, 1988; Part D, pp 303−393.

(5) (a) Sessler, J. S.; Wang, B.; Springs, S. L.; Brown, C. T. In *Comprehensive Supramolecular Chemistry*; Atwood, J. L., Davies, J. E. D., MacNicol, D. D., Vögtle, F., Eds.; Pergamon: New York, 1996; Chapter 9. (b) Hayashi, T.; Ogoshi, H. *Chem. Soc. Rev*. **1997**, *26*, 355. (c) Ward, M. W. *Chem. Soc. Rev*. **1997**, *26*, 365.

(6) (a) Gust D.; Moore, T. A. In *The Porphyrin Handbook*; Kadish, K. M., Smith, K. M., Guilard, R., Eds.; Academic Press: Burlington, MA, 2000; Vol. 8, pp 153−190. (b) Imahori, H.; Sakata, Y. *Adv. Mater*. **1997**, *9*, 537. (c) Prato, M. *J. Mater. Chem.* **1997**, *7*, 1097. (d) Martín, N.; Sánchez, L.; Illescas, B.; Pérez, I. *Chem. Rev*. **1998**, *98*, 2527. (e) Diederich, F.; Gómez-López, M. *Chem. Soc. Rev*. **1999**, *28*, 263.

(7) (a) Aviram, A., Ratner, M., Eds. Molecular Electronics: Science and Technology. *Ann. N.Y. Acad. Sci*. **1998**, *852*. (b) *Molecular Switches*; Feringa, B. L., Ed.; Wiley-VCH GmbH: Weinheim, Germany, 2001.

(8) Lindoy, L. F.; Atkinson, I. M. *Self-Assembly in Supramolecular Systems*; Royal Society of Chemistry: Cambridge, UK, 2000.

(9) (a) Kroto, H. W.; Heath, J. R.; O'Brien, S. C.; Curl, R. F.; Smalley, R. E. *Nature* **1985**, *318*, 162. (b) Kratschmer, W.; Lamb, L. D.; Fostiropoulos, F.; Huffman, D. R. *Nature* **1990**, *347*, 345. (c) *Fullerene and Related Structures*; Hirsch, A., Ed.; Springer: Berlin, Germany, 1999; Vol. 199.

(10) (a) Allemand, P. M.; Koch, A.; Wudl, F.; Rubin, Y.; Diederich, F.; Alvarez, M. M.; Anz, S. J.; Whetten, R. L. *J. Am. Chem. Soc*. **1991**, *113*, 1050. (b) Xie, Q.; Perez-Cordero, E.; Echegoyen, L. *J. Am. Chem. Soc*. **1992**, *114*, 3978.

(11) (a) Imahori, H.; Hagiwara, K.; Akiyama, T.; Akoi, M.; Taniguchi, S.; Okada, S.; Shirakawa, M.; Sakata, Y. *Chem. Phys. Lett*. **1996**, *263*, 545. (b) Guldi, D. M.; Asmus, K. D. *J. Am. Chem. Soc*. **1997**, *119*, 5744. (c) Imahori, H.; El-Khouly, M. E.; Fujitsuka, M.; Ito, O.; Sakata, Y.; Fukuzumi, S. *J. Phys. Chem. A* **2001**, *105*, 325.

(12) (a) D'Souza, F.; Deviprasad, G. R.; El-Khouly, M. E.; Fujitsuka, M.; Ito, O. *J. Am. Chem. Soc*. **2001**, *123*, 5277. (b) D'Souza, F.; Gadde, S.; Zandler, M. E.; Itou, M.; Araki, Y.; Ito, O. *Chem. Commun*. **2004**, 2276. (c) D'Souza, F.; Deviprasad, G. R.; Zandler, M. E.; El-Khouly, M. E.; Fujitsuka, M.; Ito, O. *J. Phys. Chem. A* **2003**, *107*, 4801. (d) D'Souza, F.; Chitta, R.; Gadde, S.; Zandler, M. E.; Sandanayaka, A. S. D.; Araki, Y.; Ito, O. *Chem. Commun*. **2005**, 1279.

(13) D'Souza, F.; Chitta, R.; Gadde, S.; Zandler, M. E.; Sandanayaka, A. S. D.; Araki, Y.; Ito, O. *Chem. Eur. J*. **2005**, *11*, 4416.

(14) D'Souza, F.; El-Khouly, M. E.; Gadde, S.; McCarty, A. L.; Karr, P. A.; Zandler, M. E.; Araki, Y.; Ito, O. *J. Phys. Chem. B* **2005**, *109*, 10107.

(15) *The Porphyrin Handbook*; Kadish, K. M., Smith, K. M., Guilard, R., Eds.; Academic Press: Burlington, MA, 2000; Vols. 1−10.

(16) Smith, K. M. *Porphyrins and Metalloporphyrins*; Elsevier: New York, 1977.

(17) (a) D'Souza, F.; Hsieh, Y.-Y.; Deviprasad, G. R. *Inorg. Chem*. **1996**, *35*, 5747. (b) Nappa, M.; Valentine, J. S. *J. Am. Chem. Soc*. **1978**, *100*, 5075. (c) Miller, J. R.; Dorough, G. D. *J. Am. Chem. Soc*. **1952**, *74*, 3977. (d) Kadish, K. M.; Shiue, L. R. *Inorg. Chem*. **1982**, *21*, 1112.

(18) (a) Benesi, H. A.; Hildebrand, J. H. *J. Am. Chem. Soc*. **1949**, *71*, 2703. (b) Tsukube, H.; Furuta, H.; Odani, A.; Takeda, Y.; Kudo, Y.; Inoue, Y.; Liu, Y.; Sakamoto, H.; Kimura, K. In *Comprehensive Supramolecular Chemistry*; Atwood, J. L., Davies, J. E. D., Macnicol, D. D., Vogtle, F., Eds.; Elsevier Science Inc.: New York, 1996; Vol. 8.

(19) Solladiè, N.; Walther, M. E.; Herschbach, H.; Leize, E.; Dorsselaer, A. V.; Figueira Duarte, T M.; Nierengarten, J.-F. *Tetrahedron* **2006**, *62*, 1979.

(20) Zandler, M. E.; D'Souza, F. *C. R. Chemie*, **2006**, in press.

(21) Chitta, R.; Rogers, L. M.; Wanklyn, A.; Karr, P. A.; Kahol, P. K.; Zandler, M. E.; D'Souza, F. *Inorg. Chem*. **2004**, *43*, 6969.

(22) (a) Rehm, D.; Weller, A. *Isr. J. Chem.* **1970**, *7*, 259. (b) Mataga, N.; Miyasaka, H. In *Electron Transfer*; Jortner, J., Bixon, M., Eds.; John Wiley & Sons: New York, 1999; Part 2, pp 431−496.

(23) (a) D'Souza, F.; Gadde, S.; Zandler, M. E.; Arkady, K.; El-Khouly, M. E.; Fujitsuka, M.; Ito, O. *J. Phys. Chem. A* **2002**, *106*, 12393. (b) El-Khouly, M. E.; Araki, Y.; Ito, O.; Gadde, S.; McCarty, A. L.; Karr, P. A.; Zandler, M. E.; D'Souza, F. *PhysChemPhys* **2005**, *7*, 3163.

(24) (a) Harriman, A.; Neta, P.; Richoux, M.-C. *J. Phys. Chem*. **1986**, *90*, 3444. (b) Skillman, A. G.; Collins, J. R.; Loew, G. H. *J. Am Chem. Soc*. **1992**, *114*, 9538.

(25) Nojiri, T.; Watanabe, A.; Ito, O. *J. Phys. Chem. A* **1998**, *102*, 5215.

(26) (a) Ghosh, H. N.; Pal, H.; Sapre, A. V.; Mittal J. P. *J. Am. Chem. Soc*. **1993**, *115*, 11722. (b) Fujitsuka, M.; Ito, O.; Yamashiro, T.; Aso, Y.; Otsubo, T. *J. Phys. Chem. A* **2000**, *104*, 4876.

(27) Kryatova, O. P.; Kolchinski, A. G.; Rybak-Akimova, E. V. *Tetrahedron* **2003**, *59*, 231.

(28) Lindsey, J. S.; Woodford, J. N. *Inorg. Chem*. **1995**, *34*, 1063.

(29) *Gaussian 03*, Revision B-04; Gaussian, Inc.: Pittsburgh, PA, 2003.

(30) (a) Matsumoto, K.; Fujitsuka, M.; Sato, T.; Onodera, S.; Ito, O. *J. Phys. Chem. B* **2000**, *104*, 11632. (b) Komamine, S.; Fujitsuka, M.; Ito, O.; Morikawa, K.; Miyata, T.; Ohno, T. *J. Phys. Chem. A* **2000**, *104*, 11497. (c) Yamazaki, M.; Araki, Y.; Fujitsuka, M.; Ito, O. *J. Phys. Chem. A* **2001**, *105*, 8615.